Available online at www.sciencedirect.com
ScienceDirect
Journal of the European Ceramic Society 28 (2008) 1043–1048
www.elsevier.com/locate/jeurceramsoc

Water vapor corrosion behavior of porous silicon carbide membrane support

Manabu Fukushima*, You Zhou, Yu-Ichi Yoshizawa, Kiyoshi Hirao

National Institute of Advanced Industrial Science and Technology (AIST), 2266-98 Shimo-Shidami, Moriyama-ku, Nagoya, Aichi 463-8560, Japan

Available online 26 October 2007

Abstract

High-temperature water vapor corrosion of porous silicon carbide with and without additive alumina and its microstructural feature were investigated to examine the corrosion resistance of porous membrane supports for hydrogen production by steam modification of methane. Corrosion test was performed under similar condition as hydrogen production reaction occurred at 600 and 1000 °C, 4 atm (0.4 MPa) and 3/1 = H_2O/N_2 where nitrogen gas was substituted for methane. In the corrosion at 600 °C, the alumina-doped support showed weight gain of 1.3 mg/cm^2, while the undoped support showed weight gain of 0.7 mg/cm^2. In the alumina-doped support, pore growth was observed because of the coalescence among oxidized fine particles. In contrast, the pore size of the supports without alumina was slightly reduced, due to thin silica layer formed on the SiC particle. In the corrosion at 1000 °C, the almost complete conversion to silica and the densification of silica were found. The densification of silica was due to the viscous flow sintering of silica under water vapor.

Keywords: Porosity; Corrosion; SiC; Membrane

1. Introduction

Hydrogen has played an important role in many fields and has been expected as an alternative clean energy source to replace fossil fuels, which have created a great interest in developing economical and effective methods for hydrogen production.

The following production reaction of hydrogen by the steam reforming of methane is the most typical.

$$CH_4 + H_2O \leftrightarrow 3H_2 + CO \quad (\Delta E = 206.0\,kJ/mol) \qquad (1)$$

In order to achieve sufficient hydrogen production, high temperature around 800–1000 °C and pressurized conditions (3–4 atm) are required, since this process has been limited by thermodynamic equilibrium. The improvement of energy efficiency and the cost reduction in the production process are still important issues.

High-temperature membrane reactor may be a possible method to solve the above problems. If hydrogen is continuously removed from the reaction zone through membrane, the equilibrium of the reaction moves toward hydrogen production, which can improve the conversion efficiency and decrease the reaction temperature to 500–600 °C.[1,2] Due to cost, high mechanical strength, sharp pore size distribution and good thermal and chemical stability in a water vapor environment, ceramic materials have recently gathered a considerable interest as membrane reactors. Silica or γ-alumina-based membrane coated on α-alumina membrane support is most typical.[3–7] However, the corrosion resistance of these oxides against high-temperature water vapor is a very important issue.

Compared to oxide ceramics, silicon carbide (SiC) has a low self-diffusion coefficient, better thermal shock resistance and excellent thermal stability. This strongly suggests that SiC may be useful as a membrane or a membrane support in hydrogen production. Suwanmethanond et al.[8] and Lin[9] have developed the porous SiC membrane support with alumina. We also reported the fabrication of porous SiC with submicrometer pore and porosities of 30–40%, and the effect of additive alumina on pore size.[10]

For the corrosion of SiC under high-temperature water vapor, many systematic studies have been carried out for dense materials.[11–15] They reported the relationship among atmosphere, flow rate, partial pressure, temperature, thickness of silica scale and the recession of Si–OH gas. Our report about corrosion indicated that the corrosion under normal pressure

* Corresponding author. Tel.: +81 52 736 7161; fax: +81 52 736 7405.
E-mail address: manabu-fukushima@aist.go.jp (M. Fukushima).

0955-2219/$ – see front matter © 2007 Elsevier Ltd. All rights reserved.
doi:10.1016/j.jeurceramsoc.2007.09.023

Table 1
Composition and properties of porous SiC

Sintering temperature (°C)	Composition	Sample	Porosity	Peak pore size (nm)	BET surface area (m^2/g)
1800	$SiC/Al_2O_3 = 100/0$	SC	37	410	2.1
	$SiC/Al_2O_3 = 96/4$	SCA	34	89	5.7

was affected by grain size of SiC and fabrication route.[16] These previous studies suggest that the conditions of corrosion test and the property of SiC are greatly related with its corrosion. However, the corrosion of porous SiC membrane support under similar condition to the hydrogen production has not been investigated. Especially, the changes of pore size and porosity by corrosion should be studied, because these can affect hydrogen permeability. In this paper, the corrosion of SiC membrane supports under similar condition to hydrogen production, and the changes of pore size were investigated with mercury porosimetry, scanning electron microscopy (SEM) and X-ray photoelectron spectroscopy (XPS).

2. Experimental procedure

High purity β-SiC (Ibiden Co. Ltd., Japan) powder with an average particle size of 0.30 μm was used as a raw material. As the additive, α-Al_2O_3 (Taimei Chemicals Co. Ltd., Japan) with an average particle size of 0.20 μm was used. The mixtures with weight ratios of $Al_2O_3/SiC = 0/100$ and 4/96 were blended in ethanol for 1 h by using a planetary mill. The powder compacts were formed without any binder by using a steel mold, and then treated with cold isostatic press (CIP) at 400 MPa. The green compacts were sintered at 1800 °C for 2 h under Ar gas flow. Hereafter, these sintered specimens are referred as SC ($Al_2O_3/SiC = 0/100$) and SCA ($Al_2O_3/SiC = 4/96$), respectively, according to the additive. Detail process factors to affect microstructure have been reported elsewhere.[10] The properties of the obtained porous SiC specimens are illustrated in Table 1.

The water vapor corrosion was performed using a Corrosion Testing Machine at Japan Ultra High Temperature Materials Research Center. The corrosion tests were performed at 600 or 1000 °C and holding period was 100 h. Flow rate was 30 mm/min. Nitrogen gas was flowed to above testing temperature and then, mixed gas of N_2 and H_2O was introduced for the holding period. The partial pressure of water vapor was kept at 1/3 (N_2/H_2O) under 4 atm.

For the analyses of corrosion behavior, porosity, surface area, pore size distribution, SEM and XPS were used. Open porosity was measured by Archimedes method with water displacement.[17] Specific surface area determined from BET analysis (Brunauer, Emmet and Teller) was measured by nitrogen adsorption (Yuasa Ionics Inc., Autosorb, Osaka, Japan).[18] The pore size distributions before and after corrosion were characterized by mercury porosimetry (Yuasa Ionics Inc., PoreMaster-GT, Osaka, Japan). The microstructures before and after water vapor corrosion were observed using a SEM (JEOL-6330F, Tokyo, Japan). XPS was used for the structural investigation of the surface of the specimens before and after vapor corrosion. The measurements were operated around 1.3×10^{-8} Pa and using Mg Kα radiation. The C (1s) spectra for an internal reference (284.6 eV in hydrocarbon) were used as the calibration of binding energy.

3. Results and discussion

Dimensional changes, weight changes, porosities and conversion to silica after vapor corrosion are listed in Table 2. The weight gain of the SCA was found to be larger than that of the SC for both corrosion temperatures. The corrosion at 1000 °C resulted in dramatic weight gain. According to the following equation, weight gain due to the conversion to silica is represented:

$$SiC + 3H_2O(g) \rightarrow SiO_2 + 3H_2(g) + CO(g) \quad (2)$$

The conversion rate from SiC to silica was calculated by the weight gain. The complete conversion to silica accompanies with the weight gain of 50 mass%. The conversion rate can be worked out by the measured weight gain/the weight gain (50 mass% for the SC or 48 mass% for the SCA) of complete conversion. In corrosion at 1000 °C, the almost complete conversion was observed. And the expansion was also found, which meant that formed silica by corrosion had larger volume due to lower density than SiC. Then, the porosity of the SC and the SCA decreased to 36 and 32% at 600 °C, and then dramatically decreased to 4 and 7% at 1000 °C, suggesting the progress of densification of silica.

Fig. 1 shows the BET surface area before and after corrosion. The SC and the SCA before corrosion had surface area of 2.1 and 5.7 m^2/g, respectively. The SCA seems to contain the higher content of fine particles than the SC. By corrosion at 600 °C, those surface areas decreased to 1.9 and 4.1 m^2/g, which

Table 2
Dimensional changes, specific weight change (g/cm^2), porosity and conversion rate of the porous SiC after vapor corrosion

Sample	Corrosion temperature (°C)	Dimensional change (%)	Specific weight change (mg/cm^2)	Porosity (%)	Conversion to silica (%)
SC	600	−0.6	0.7	36	0.7
SCA		−2.1	1.3	32	1.1
SC	1000	+17.2	93.9	4	95.7
SCA		+18.6	111.4	7	97.5

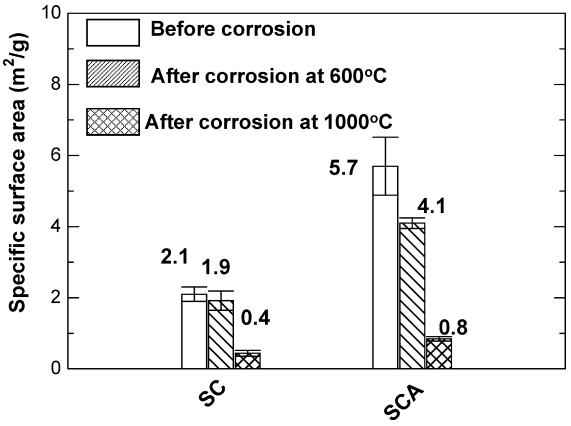

Fig. 1. Changes of BET surface area of the porous SiC before and after vapor corrosion.

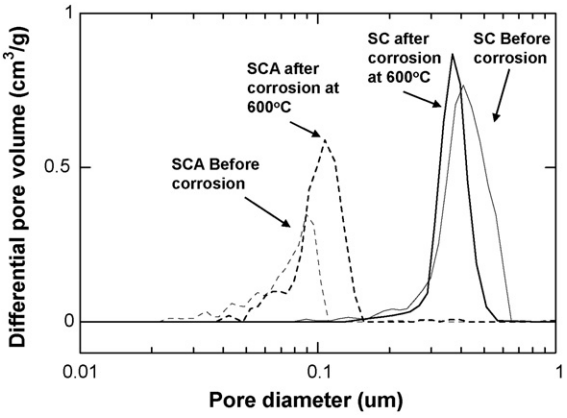

Fig. 2. Pore size distribution of the porous SiC before and after vapor corrosion.

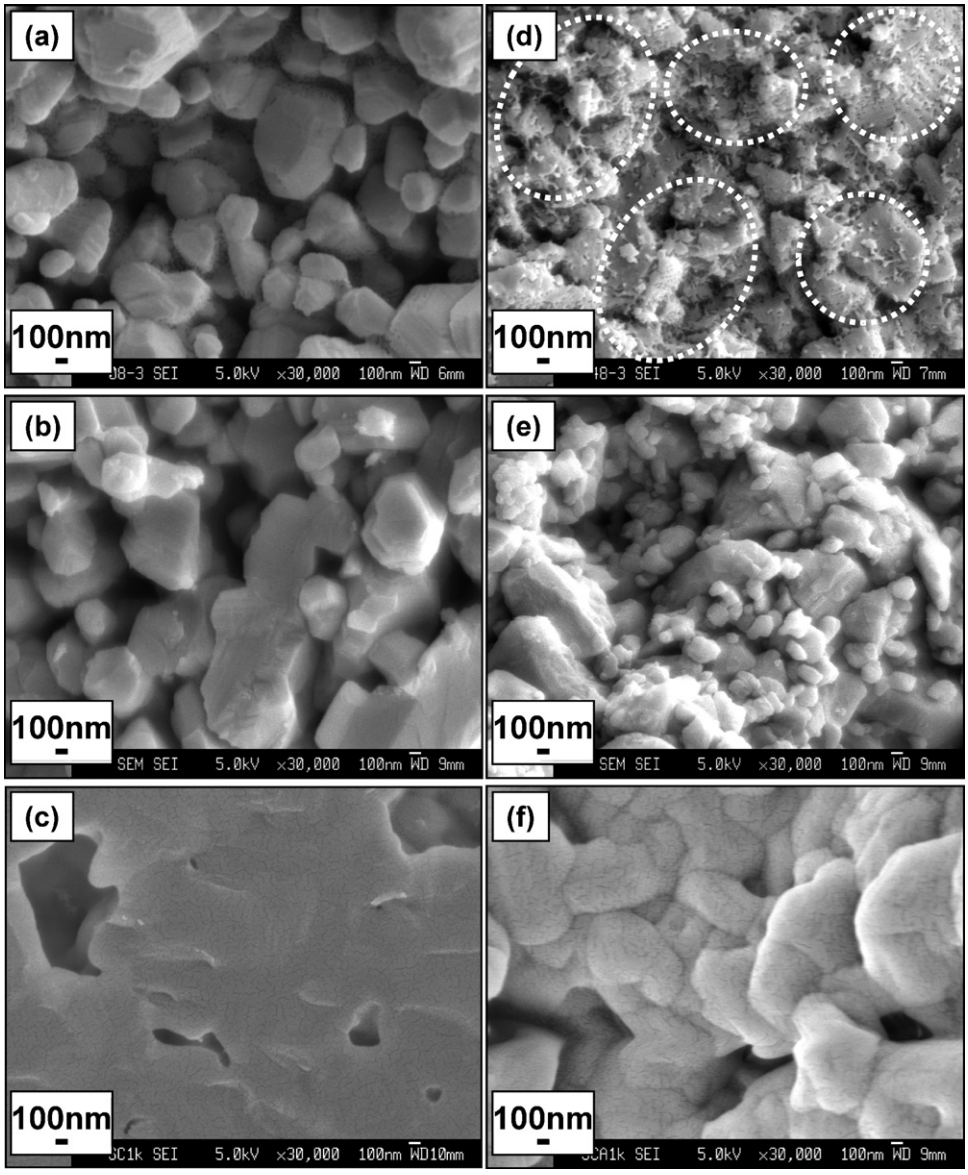

Fig. 3. FE-SEM micrographs of the fractured SC and SCA: (a and d) as-received; (b and e) after vapor corrosion at 600 °C and (c and f) at 1000 °C.

were about 90 and 72% of initial surface area, respectively. Surface area further decreased with the increase of corrosion temperature. This is found to be consistent with the decrease of porosity (Table 2). The surface area of macroporous material is generally affected by particle size and porosity. The decrease of surface area suggests the decrease of the number of fine particles, the decrease of porosity and the increase of particle size.

Fig. 2 shows the pore size distributions of the SC and the SCA before and after vapor corrosion. The pore sizes of as-received SC and SCA were distributed in the range of 0.16–0.65 and 0.02–0.11 μm, respectively. By corrosion at 600 °C, the pore size of the SC decreased to 0.16–0.57 μm, while the pore size of the SCA increased to 0.04–0.16 μm. It can be seen that the pore size of 0.08 μm in the SC is reduced and the size of 0.02–0.05 μm in the SCA is enlarged by corrosion. In addition, small pore around 0.02–0.04 μm in the SCA disappeared, though that was much smaller change.

These changes are considered to be available range as hydrogen production of membrane support, which requires the retention of submicrometer pore around 500–600 °C. In contrast, by corrosion at 1000 °C, no pore could be monitored by mercury porosimetry, although porosity was slightly detected by Archimedes method (Table 2). The observed reduction of porosity and pore suggests that the porous SiC at 1000 °C should not be utilized.

Fig. 3 shows the FE-SEM micrographs of the fractured surface for the SC (Fig. 4(a–c)) and the SCA (Fig. 4(d–f)) before and after vapor corrosion at 600 and 1000 °C. In (a) and (d) micrographs for as-received specimens, particle size and pore size were varied by the addition of alumina, which was due to different mass transfer during sintering. In the undoped specimen, surface diffusion was main mass transfer pass, which caused enlarged pore and grain coarsening. In contrast, for the alumina-doped SiC, SiO_2–Al_2O_3 liquid phase between silica on the particle surface and additive alumina was formed during sintering, leading to the prevention of pore growth and grain coarsening. These partial sintering behaviors were previously confirmed by TEM–EDS analysis and elemental mapping.[10]

The micrograph (b) of the SC after corrosion at 600 °C revealed that the microstructure of the SC was not significantly different from that (a) of as-received specimen. In contrast, seen from the (d) and (e), by corrosion, the observed fine SiC particles (as indicated by circles) disappeared or changed to spherical shape. On the other hand, in corrosion at 1000 °C, microstructures dramatically changed. The fine particles completely disappeared, and grain coarsening was observed. Then, the SCA was found to have appreciable grain boundary.

Fig. 4 illustrates the (A) Si (2p) and (B) O (1s) spectra of the SCA before and after vapor corrosion. As seen from the Si (2p) spectra, the peak due to silicon carbide before corrosion, two peaks ascribed to silicon oxycarbide and silica after corrosion at 600 °C and the peak due to silica after corrosion at 1000 °C were detected, respectively.[19,20] At 600 °C, the complete conversion to silica in the Eq. (2) was not found to completely perform even at surface detected by XPS. The surface composition of the SC

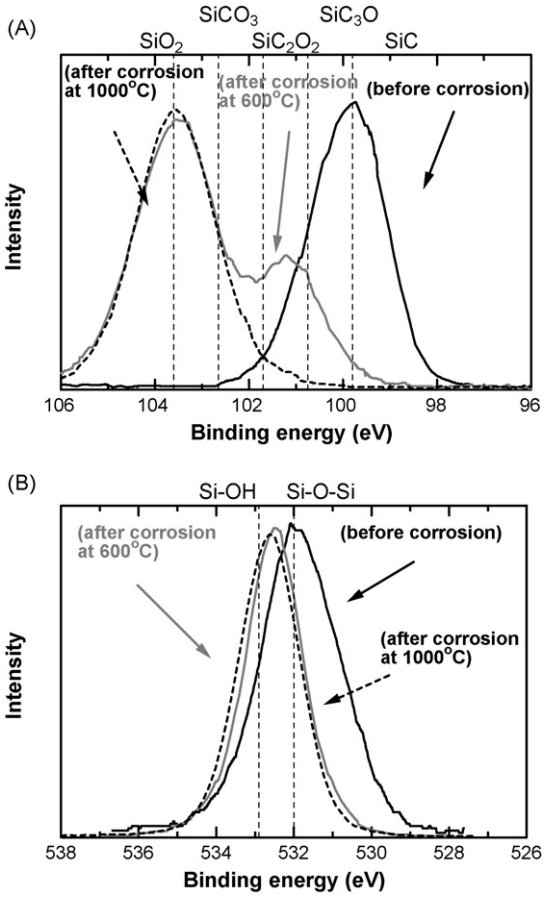

Fig. 4. (A) Si (2p) and (B) O (1s) XPS spectra of the SCA before and after water vapor corrosion.

and the SCA were nearly same; $SiC_{0.20}O_{1.60}$ and $SiC_{0.18}O_{1.64}$, respectively, which was calculated by the ratio of the area in the peak deconvolution. This suggests that the rate of corrosion may be nearly equal for both specimens.

In the O (1s) spectra, the peak due to Si–O–Si (siloxane) in the specimen before corrosion was monitored. This is due to siloxane in thin silica layer on the surface of SiC particle. After corrosion, peak shifted to higher binding energy, which was ascribed to the formation of Si–OH (silanol) group.[21,22] Silanol group can be easily produced by the cession of siloxane bonds under high-temperature water vapor, according to the following equation[23]:

$$\equiv\text{Si–O–Si–} + \text{H}_2\text{O} \rightarrow 2 \equiv \text{Si–OH} \quad (3)$$

Oxycarbide or silica, detected by Si-XPS spectra, may accompany with silanol group on their terminal site.

The decrease of surface area, the changes of pore size and the formation of Si–OH group were monitored by corrosion. Here, we discuss the relationship among these phenomena. First, in the SC, the particle size after corrosion at 600 °C was almost similar with that of the as-received specimen (see Fig. 3). However, surface area and pore size were slightly reduced. This means that the thin silica layer on the SiC particle is formed by corrosion, namely, apparent particle size is slightly enlarged due to lower density of silica than that of SiC. This can lead to the narrower

pore size and the decrease of surface area due to slight increase of particle size.

In contrast, for the SCA after corrosion at 600 °C, pore size was enlarged and small pore around 0.02–0.04 μm was closed (see Fig. 2). Then, fine particles less than at least 100 nm (as observed in Fig. 3d) disappeared, suggesting that some fine particles completely converted to silica. In addition, the formation of silanol group was detected by XPS spectra. During vapor corrosion, the surface of SiC particle is oxidized and a silica layer is generated by Eq. (2). When the silica on the surface of particle partially accompanies with silanol groups, viscosity greatly decreases with the content of silanol.[24] Seen from the previous reports, the viscosity of silica without silanol is one to two orders of magnitude higher than that of silica with much slight silanol content (0.01 mass%).[24,25] The silica layer or fine particles with silanol may gradually gather toward neck area due to low viscosity and surface tension. This should result in the pore growth, the coalescence with fine particle and the closure of small pore, which is consistent with the decrease of surface area.

The pore of the SC was reduced and that of the SCA was enlarged, which were both due to the formation of silica layer. The coarse particle of the SC has silica layer on the surface, which can reduce pore size. In contrast, some fine particles of the SCA may be completely oxidized. The complete corrosion of fine particles leads to the grain coarsening by their gathering due to low viscosity, closure of small pore around 0.02–0.04 μm and then pore growth.

During the corrosion at 1000 °C, the dramatic decrease of porosity, the almost complete conversion to silica and the densification of silica were found. The viscous flow sintering of silica under water vapor is considered to occur.[23–25] Though the porosities of both specimens were slightly different, the observed reduction of porosity suggests that the porous SiC at 1000 °C should not be utilized.

The hydrogen production reaction occurs around 800–1000 °C. However, by using membrane reactor, its reaction temperature can be lowered to 500–600 °C. In the corrosion test at 600 °C, the submicrometer pore required for membrane support was retained, although slight changes were monitored. Thus, this study suggests that porous SiC for hydrogen production by membrane can be available.

4. Conclusion

The corrosion of porous SiC with and without alumina was performed under similar condition to hydrogen production reaction (at 600 and 1000 °C, 4 atm (0.4 MPa) and partial pressure of 75% H_2O), and the role of microstructures on corrosion behavior was investigated.

By the corrosion at 600 °C, the pore size of supports with alumina showed the slight increase. This was considered to be due to the coalescence among oxidized fine particles. In the support without alumina, pore size was reduced by corrosion at 600 °C, which was due to thin silica layer formed on the SiC particle. Though the changes of pore size were monitored, pore sizes after corrosion at 600 °C were remained in the range of submicrometer for both supports. In the corrosion at 1000 °C, the almost complete conversion to silica and the densification due to the viscous flow sintering of silica occurred on both supports, which suggested that porous SiC at 1000 °C should not be used.

Acknowledgement

The authors gratefully acknowledge financial support from NEDO.

References

1. Kikuchi, E., Nemoto, Y., Kajiwara, M., Uemiya, S. and Koji, T., Steam reforming of methane in membrane reactors: comparison of electroless-plating and CVD membranes and catalyst packing modes. *Catal. Today*, 2000, **56**, 75–81.
2. Jarosch, K. and Lasa, H. I., Novel riser simulator for methane reforming using high-temperature membranes. *Chem. Eng. Sci.*, 1999, **54**, 1455–1460.
3. Zahir, M. H., Sato, K. and Iwamoto, Y., Development of hydrothermally stable sol–gel derived La_2O_3-doped Ga_2O_3–Al_2O_3 composite mesoporous membrane. *J. Membr. Sci.*, 2005, **247**, 95–101.
4. Yoshida, K., Hirano, Y., Fujii, H., Tsuru, T. and Asaeda, M., Hydrothermal stability and performance of silica–zirconia membranes for hydrogen separation in hydrothermal conditions". *J. Chem. Eng. Jpn.*, 2001, **34**, 523–530.
5. Kusakabe, K., Li, Z. Y., Maeda, H. and Morooka, S., Preparation of supported composite membrane by pyrolysis of polycarbosilane for gas separation at high temperature. *J. Membr. Sci.*, 1995, **103**, 175–180.
6. Lin, Y.-S. and Burggraaf, A. J., Preparation and characterization of high-temperature thermally stable alumina composite membrane. *J. Am. Ceram. Soc.*, 1991, **74**, 219–224.
7. Sea, B. K., Kusakabe, K. and Morooka, S., Pore size control and gas permeation kinetics of silica membranes by pyrolysis of phenyl-substituted ethoxysilanes with cross-flow through a porous support wall. *J. Membr. Sci.*, 1997, **130**, 41–52.
8. Suwanmethanond, V., Goo, E., Liu, P. K. T., Johnston, G., Sahimi, M. and Tsotsis, T. T., Porous silicon carbide sintered substrates for high-temperature membranes. *Ind. Eng. Chem. Res.*, 2000, **39**, 3264–3271.
9. Lin, P.-K. and Tsai, D.-S., Preparation and analysis of a silicon carbide composite membrane. *J. Am. Ceram. Soc.*, 1997, **80**, 365–372.
10. Fukushima, M., Zhou, Y., Iwamoto, Y., Yamazaki, S., Nagano, T., Miyazaki, H. *et al.*, Microstructural characterization of porous silicon carbide membrane support with and without alumina additive. *J. Am. Ceram. Soc.*, 2006, **89**, 1523–1529.
11. Robinson, R. C. and Smialek, J. L., SiC recession caused by SiO_2 scale volatility under combustion conditions: I. Experimental results and empirical model. *J. Am. Ceram. Soc.*, 1999, **82**, 1817–1825.
12. Opila, E. J., Smialek, J. L., Robinson, R. C., Fox, D. S. and Jacobson, N. S., SiC recession caused by SiO2 scale volatility under combustion conditions: II. Thermodynamics and gaseous-diffusion model. *J. Am. Ceram. Soc.*, 1999, **82**, 1826–1834.
13. Opila, E. J., Variation of the oxidation rate of silicon carbide with water vapor pressure. *J. Am. Ceram. Soc.*, 1999, **82**, 625–636.
14. Tortorelli, P. F. and More, K. L., Effects of high water vapor pressure on oxidation of silicon carbide at 1200 °C. *J. Am. Ceram. Soc.*, 2003, **86**, 1249–1255.
15. More, K. L., Tortorelli, P. F., Walker, L. R., Miriyala, N., Price, J. R. and Roode, M. V., High-temperature stability of SiC-based composites in high-water vapor–pressure environments. *J. Am. Ceram. Soc.*, 2003, **86**, 1272–1281.
16. Fukushima, M., Zhou, H., Yoshizawa, Y. and Hirao, K., Oxidation behavior of porous silicon carbide ceramics under water vapor below 1000 °C and their microstructural characterization. *J. Ceram. Soc. Jpn.*, 2006, **114**, 1155–1159.
17. Jones, J. T. and Berard, M. F., *Ceramics—Industrial Processing and Testing*. The Iowa State University Press, Ames, 1993, 172–174.

18. Brunauer, S., Emmett, P. H. and Teller, E., Adsorption of gases in multimolecular layers. *J. Am. Chem. Soc.*, 1938, **60**, 309–319.
19. Belot, V., Leclercq, D., Mutin, P. H. and Vioux, A., Preparation and structure of silicon oxycarbide glasses derived from polysiloxane precursors. *J. Sol-Gel Sci. Technol.*, 1997, **8**, 327–330.
20. Soraru, G. D., Andrea, G. D. and Glisenti, A., XPS characterization of gel-derived silicon oxycarbide glasses. *Mater. Lett.*, 1996, **27**, 1–5.
21. Takadama, H., Kim, H.-M., Kokubo, T. and Nakamura, T., X-ray photoelectron spectroscopy study on the process of apatite formation on a sodium silicate glass in simulated body fluid. *J. Am. Ceram. Soc.*, 2002, **85**, 1933–1936.
22. Sprenger, D., Bach, H., Meisel, W. and Gu¨tlich, P., XPS study of leached glass. *J. Non-Cryst. Solids*, 1990, **126**, 111–129.
23. Scholze, H., Gases and water in glass. *Glass Ind.*, 1966, **47**, 622–628.
24. Hetherington, G., Jack, K. H. and Kennedy, J. C., The viscosity of vitreous silica. *Phys. Chem. Glasses*, 1964, **5**, 130–136.
25. Hirao, K., Yasuoka, M. and Kanzaki, S., Effect of water vapor pressure on the viscous sintering of mullite. *J. Ceram. Soc. Jpn.*, 1995, **103**, 1172–1176.